Taylor & Francis
Taylor & Francis Group

RESEARCH PAPER

Check for updates

Trichostatin A decreases the levels of MeCP2 expression and phosphorylation and increases its chromatin binding affinity

Katrina V. Good[a,†], Alexia Martínez de Paz[a,†], Monica Tyagi[a,†], Manjinder S. Cheema[a], Anita A. Thambirajah[a,b], Taylor L. Gretzinger[a], Gilda Stefanelli[c], Robert L. Chow[d], Oliver Krupke[d], Michael Hendzel[e,f], Kristal Missiaen[f], Alan Underhill[f], Nicoletta Landsberger[c], and Juan Ausió[a]

[a]Department of Biochemistry and Microbiology, University of Victoria, Victoria, BC, V8W 3P6, Canada; [b]Douglas Hospital Research Center, Department of Psychiatry, McGill University, Montréal, Québec H3G 1Y6, Canada; [c]Department of Medical Biotechnology and Translational Medicine, University of Milan, Milan, Italy; [d]Department of Biology, University of Victoria, Victoria, BC, V8W 3P6, Canada; [e]Department of Cell Biology, Faculty of Medicine and Dentistry, University of Alberta, Edmonton, Alberta, Canada; [f]Department of Oncology and Department of Cell Biology, Faculty of Medicine and Dentistry, University of Alberta, Edmonton, Alberta, Canada

ABSTRACT

MeCP2 binds to methylated DNA in a chromatin context and has an important role in cancer and brain development and function. Histone deacetylase (HDAC) inhibitors are currently being used to palliate many cancer and neurological disorders. Yet, the molecular mechanisms involved are not well known for the most part and, in particular, the relationship between histone acetylation and MeCP2 is not well understood. In this paper, we study the effect of the HDAC inhibitor trichostatin A (TSA) on MeCP2, a protein whose dysregulation plays an important role in these diseases. We find that treatment of cells with TSA decreases the phosphorylation state of this protein and appears to result in a higher MeCP2 chromatin binding affinity. Yet, the binding dynamics with which the protein binds to DNA appear not to be significantly affected despite the chromatin reorganization resulting from the high levels of acetylation. HDAC inhibition also results in an overall decrease in MeCP2 levels of different cell lines. Moreover, we show that miR132 increases upon TSA treatment, and is one of the players involved in the observed downregulation of MeCP2.

Introduction

Methyl CpG binding protein 2 (MeCP2) is a basic DNA binding protein with preference for methylated DNA[1,2] and is highly abundant in the brain.[3] This protein functions as a transcriptional regulator by virtue of its interaction with both transcription activator and repressor complexes.[4,5] In neurons, one MeCP2 molecule is present in approximately every two nucleosomes;[6] hence, it is a very important chromosomal protein whose alterations have dire neurological consequences,[1,7] for example, Rett syndrome.[8] In other cell types and tissues, the abundance of this protein is approximately 30- to 40-fold lower than in neurons.[3] Nevertheless, its functional role in these cells is also important. Indeed, MeCP2, by virtue of its specific binding to methylated DNA, plays a very important role in cancer,[9,10] where the dysregulation of this epigenetic mark is a hallmark[11] that leads to important structural chromatin changes.[12] Moreover, *MECP2* was recently shown to be a *bona fide* oncogene,[13] which is frequently amplified in several cancer types.

Histone acetylation affects inter- and intra-nucleosome interactions[14,15] within the chromatin fiber as well as inter-chromatin fiber associations[16] and has been extensively studied in our lab over the years.[17,18]

The interaction of MeCP2 with methylated DNA on a chromatin template and the massive presence of MeCP2 in neuronal chromatin unavoidably makes it an important functional partner of histones and their posttranslational modifications (PTMs).[19] For instance, histone acetylation also plays a critical role in neurogenesis and neuronal plasticity,[20] and its levels are affected in many functional neuronal alterations.[1,21] However, the potential cross-talk between MeCP2 and histones is largely unknown and remains to be elucidated.

In particular, the regulation of MeCP2 mediated by HDAC inhibitors is very important, as such compounds are currently used both in cancer therapy[22-33] and for the treatment of several neurological disorders[34-40] to different levels of success.[41,42] Hence, understanding the molecular details of the effect(s) of such inhibitors on MeCP2 homeostasis is of major importance.

CREB and microRNAs arising from the miR132/212 cluster have also been shown to play important roles in MeCP2 homeostasis. CREB has been shown to stimulate miR132[43] and miR212[44] expression; miR212 conversely activates CREB.[44] At the same time, both mRNAs can block MeCP2 translation[43,45] and MeCP2 can repress pri-miR132/212 expression. In a similar fashion, CREB can repress MeCP2 and vice versa.[46]

CONTACT Juan Ausió ✉ jausio@uvic.ca 🖂 Department of Biochemistry and Microbiology, Petch Building 260, University of Victoria, Victoria, BC, Canada V8W 3P6.

[†]These authors have contributed equally to this work.

Several years ago, an intriguing observation was made in our lab that showed that treatment of HeLa cells with the HDAC inhibitor sodium butyrate in order to induce global genome histone acetylation resulted in a significant decrease in MeCP2.[47] While other labs have seen decreased MeCP2 with HDAC inhibition in other cell lines,[48,49] the observation remains puzzling as it is hard to explain by the 'dogma' ensuing from the initial association of MeCP2 to transcriptional repression.[50] This activity is mediated by the binding of the Sin3A-HDAC repressive complex[51] to MeCP2, and, hence, the presence of MeCP2 in the genome should result in an overall reciprocal decrease in histone acetylation, as was experimentally observed.[6] Yet, the opposite did not follow from said mechanism (i.e., HDAC inhibition did not lead to increased MeCP2). Similarly, an anti-correlation between DNA methylation and histone acetylation has been reported.[52] The current paper represents a follow up on our initial observation and it shows that the relation between histone acetylation, HDACs and MeCP2 is not as simple as originally envisaged.

To date, the most significant studies on MeCP2 have been carried out in the brain.[1] In this study, we took advantage of some mechanistic molecular information already available for MeCP2 from this tissue and analyzed it in the frame of non-neuronal cell lines. As mentioned, MeCP2 plays a critical role in cancer;[53,54] however, the detailed underlying mechanisms have not been widely studied.

Results

TSA treatment results in chromatin reorganization and MeCP2 redistribution within the nucleus without affecting the dynamics of MeCP2 association-dissociation. To follow up on our intriguing initial observation on the decrease of MeCP2 levels upon sodium butyrate treatment, and since we had originally shown that MeCP2 chromatin partitioning was minutely affected by the HDAC inhibitor treatment of the cell,[47] we decided to check first the effects of TSA (a commonly used HDAC inhibitor in recent studies)[55-57] on MeCP2 nuclear distribution and on its interactions with chromatin. To this end, we used mouse embryonic fibroblast NIH/3T3 cells because their chromatin is organized into dense pericentomeric domains[58] ("chromocenters") consisting of major and minor satellite DNA regions[59] that can be easily visualized by optical microscopy and are associated with MeCP2.[60]

The chromatin reorganization in the nucleus resulting from TSA treatment has been extensively characterized and mouse NIH/3T3 cells have been shown to provide a unique system for these kinds of analyses.[61] Fig. 1a shows an example of this in which we also monitored the distribution of MeCP2. As previously described, TSA treatment leads to chromatin decondensation that affects both the euchromatin and heterochromatin compartments. This chromatin rearrangement is mirrored by that of MeCP2, which exhibits a more diffuse distribution across the nucleus in which the chromocenters have been partially dispersed, as indicated by DAPI staining. This results in overall global opening of chromatin as visualized by the small but noticeable MNase digestion of chromatin observed in Fig. 1b. Biochemically, TSA treatment results in a redistribution and increase of both repressive and activating histone PTMs in the MNase generated SI, SE, and P chromatin fractionations[3] (Fig. 1c) without affecting their characteristic MeCP2 content.[3,47] The enrichment of these histone epigenetic marks in the nuclease-accessible SI fraction upon treatment with TSA is in agreement with our previous results.[62]
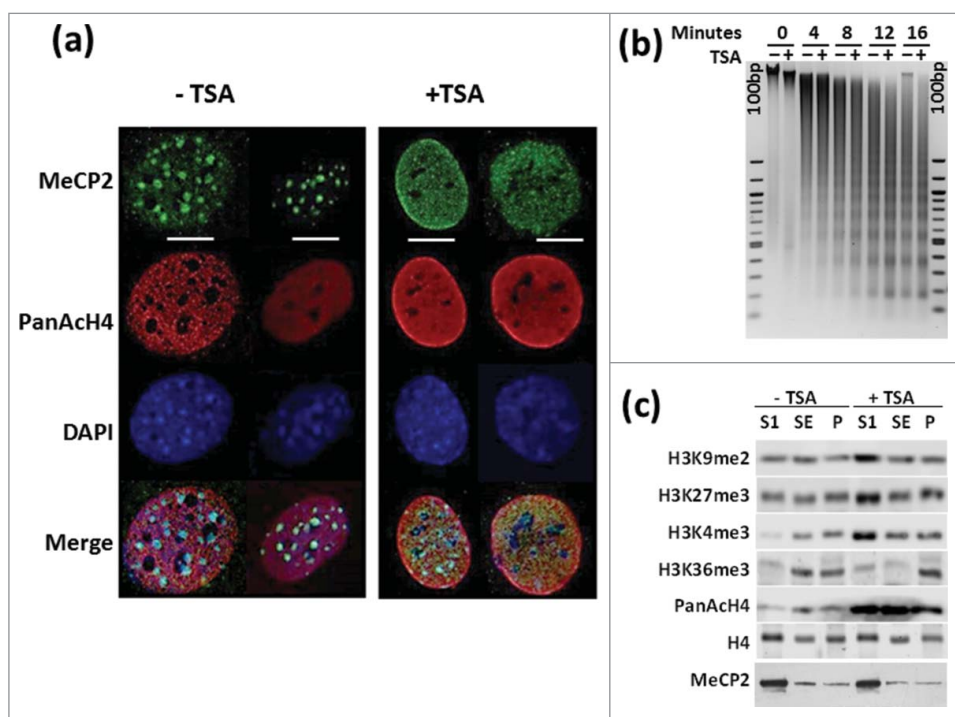

Figure 1. TSA treatment results in chromatin rearrangement. (a) Immunofluorescence analysis of MeCP2 and acetylated H4 distribution in NIH/3T3 cells +TSA and -TSA. Scale bars: 10 μm. (b) Time course microccocal nuclease digestion and (c) Western blot analysis of several histone PTMs before and after TSA treatment of the same cells. "100 bp" corresponds to a 100 bp marker. SI, SE, and P represent the chromatin fractions obtained upon micrococcal nuclease digestion as described in 3.
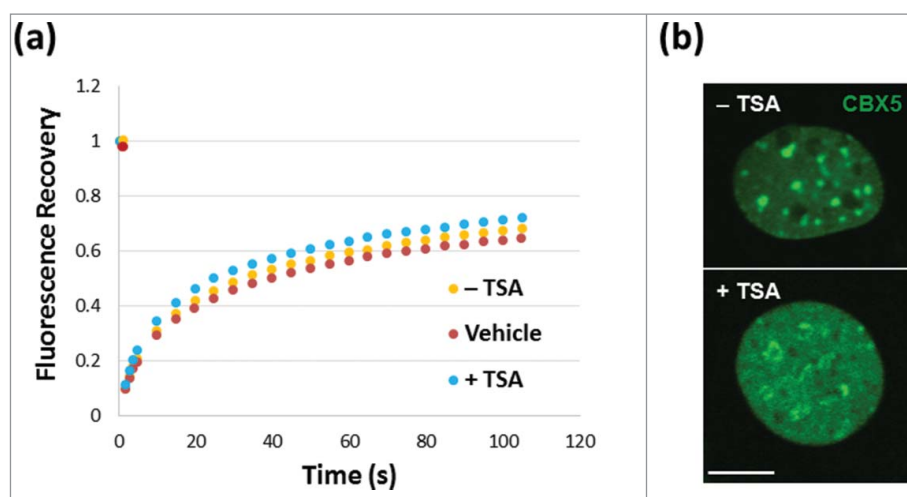
Figure 2. FRAP analysis of NIH/3T3 cells. (a) Untransfected NIH/3T3 cells in the presence (red)/absence (orange) of DMSO controls or transfected with GFP-MeCP2 (blue). (a) Green fluorescence analysis of the distribution of chromobox homolog (CBX5) in the nuclei used for the analyses shown in (a), with (+) or without (−) TSA treatment. Scale bar: 10 μm.

We then wanted to analyze how all of this affects the interaction of MeCP2 with chromatin. In this regard, it is noteworthy that despite the nuclear chromatin relocalization of MeCP2 observed in Fig. 1a, fluorescence recovery after photobleaching (FRAP) (Fig. 2a) clearly indicates that TSA treatment does not affect the dynamics with which MeCP2 associates and dissociates from chromatin. To ensure that the cells being analyzed by FRAP had undergone TSA treatment, cells were visualized using a chromobox homolog 5 (CBX5) antibody. CBX5 binds to H3K9me present in heterochromatin and, as seen in Fig. 2b, has undergone redistribution upon TSA treatment similar to that shown in Fig. 1a and is in agreement with Fig. 1b H3K9me2 redistribution.

TSA treatment increases MeCP2 chromatin binding affinity and decreases its global phosphorylation in NIH/3T3 cells. To gain further molecular detail on the effects of TSA on the interaction of MeCP2 with chromatin we performed ionic-strength-dependent experiments.[3] Despite the little effect of TSA treatment on the dynamics of MeCP2 binding (Fig. 2), we decided to check whether its chromatin binding affinity was affected. Indeed, MeCP2 and histone H1, which bind and compete for similar linker DNA regions, have very different binding affinities [(see Fig. 3E, in reference 3)], yet they exhibit almost identical chromatin binding dynamics (unpublished results and[63,64]). For consistency, the analysis was performed in NIH/3T3 cells grown in the presence or absence of TSA (Fig. 3). Upon treatment with different NaCl concentrations, nuclear suspensions were pelleted and MeCP2 levels were measured in both supernatant and pellet fractions. The reciprocal increase and decrease of MeCP2, respectively, provided validation of experimental success. We found that TSA substantially increased the binding affinity of MeCP2 to chromatin. This was unexpected, as previous results from our lab had shown that, in vitro, histone acetylation did not affect the binding of recombinant MeCP2 to the nucleosome.[47]

The obvious candidate for the intriguing in vivo results seen in Fig. 3 became MeCP2 phosphorylation.[65-67] MeCP2 is an intrinsically disordered protein and, as such, is subject to many PTMs,[7] including phosphorylation.[67] Histone phosphorylation

has been shown to globally decrease its chromatin binding affinity[68,69] and TSA has been shown to downregulate several cyclin dependent kinases (CDKs).[70]

We decided to analyze two of the most intensively characterized phosphorylation sites to date, S80-P and S421-P.[71] In neurons, S80 is constitutively phosphorylated in the resting state[72] and S421 is phosphorylated in response to neuronal activity.[69] We also decided to include S164-P, a recently described abundant developmental MeCP2 phosphorylation, which has been documented to lower its binding affinity to chromatin.[66] The results of such analyses are shown in Fig. 4. While we were not able to detect any significant change in S80 and only a relative change in S421 phosphorylation, the decrease observed in S164 suggests that MeCP2 phosphorylation reduction could be responsible for the TSA-driven increase in chromatin binding affinity (Fig. 3).
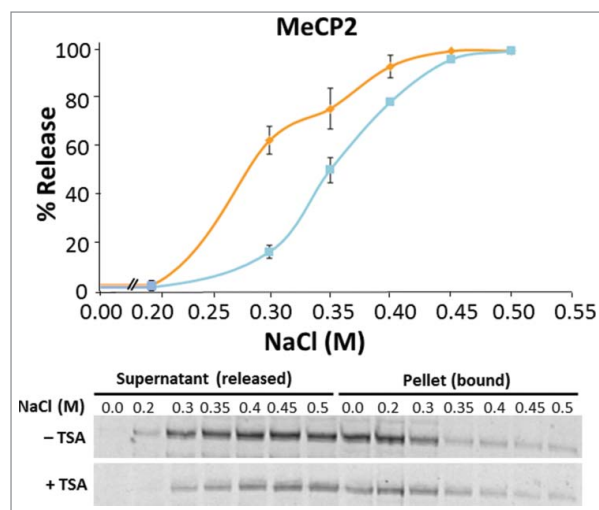

Figure 3. TSA treatment affects the binding of MeCP2 to chromatin. Salt (NaCl) extraction of MeCP2 from nuclei of untreated (orange line) and TSA treated (blue line) NIH/3T3 cells. Quantitative western blots were carried out on n = 2 independent experiments. MeCP2 levels were measured in both supernatant and pellet fractions, given that the reciprocal increase and decrease of MeCP2 represent the unbound (released) and bound fractions from cell nuclei, respectively. Data presented as mean ± SEM.
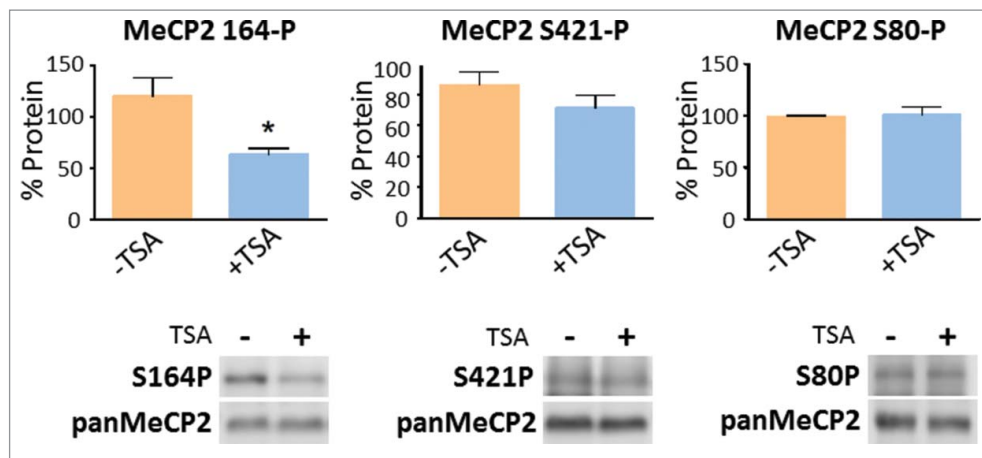
Figure 4. TSA exposure alters the levels of MeCP2 phosphorylation. Changes in the levels of MeCP2 phosphorylation at positions S80, S164, and S421, normalized to total MeCP2, both without (−) and with (+) exposure to TSA. Equal loadings of total MeCP2 (in control and treated samples) were used so that changes in the phosphorylated forms could be visualized. Westerns for total MeCP2 and each one of the corresponding phosphorylated forms were obtained from the same gel (membrane). Data represents mean ± SEM of 4 independent experiments. Mann-Whitney tests were used to calculate significance; * P value <0.05, $^{**}P$ value <0.01, $^{***}P$ value <0.001. Representative blot images are shown in greyscale black on white format.

TSA treatment decreases the level of MeCP2. TSA has the same effect in decreasing the levels of MeCP2 as previously observed when we exposed HeLa cells to sodium butyrate. Different types of mouse and human cell lines were treated (Fig. 5). The cells chosen encompass different developmental origin: human HeLa (ectoderm) and HEK293 (mesoderm), as well as mouse embryonic fibroblast NIH/3T3 (mesoderm).

As seen in Fig. 5a–b, TSA[73] treatment resulted in a decrease of MeCP2 and an increase in the levels of histone acetylation, thus recapitulating our earlier observation.[47] Treatment with TSA resulted in an approximate 30–40% decrease in MeCP2, while the level of histone acetylation increase was 2–2.5-fold. Moreover, the lower levels of MeCP2 observed are the result of a similar decrease in the levels of MeCP2 mRNA (Fig. 5c).

Therefore, we decided to analyze the potential molecular mechanism involved.

Exposure of NIH/3T3 cells to HDAC inhibition increases the expression of miR132/212. The observed decrease of MeCP2 in NIH/3T3 cells upon exposure to TSA was intriguing. Homeostasis of MeCP2 is critical, particularly in neurons, where a tight regulation of its levels is required for their proper function.[74] cAMP responsive element binding protein (CREB)-binding protein (CREB-CBP) have been involved in this process through a CREB-induced microRNA (miR132/212).[43] CBP is a highly abundant histone acetyl transferase (HAT) subunit that interacts with CREB. We reasoned that TSA treatment could decrease the levels of MeCP2 by upregulating the expression of miR132/212.
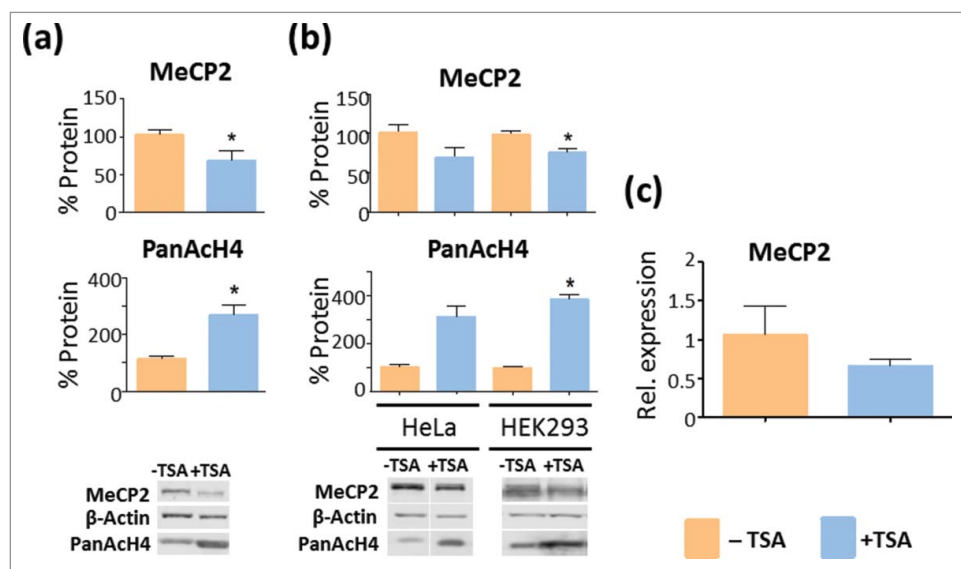

Figure 5. TSA decreases the levels of MeCP2 in different cell lines. (a) Comparison of the effects of TSA (330 nM) treatment for 24 h. on the levels of MeCP2 and histone H4 acetylation in NIH/3T3 mouse fibroblasts. (b) Effects of TSA treatment on HeLa S3 [40 ng/mL (132 nM), 12 h] and HEK293 [120 ng/mL (396 nM), 18 h]. Representative WB bands shown to be disconnected were non-adjacent signals visualized on the same membrane. (c) Quantification of MeCP2 transcripts by real-time RT-PCR of NIH/3T3 cells with and without TSA treatment. Data presented as mean ± SEM of 3–11 experiments. Unpaired two tailed t-tests were used for large sample sizes wherein normal distribution could be validated (using Shapiro-Wilk test) and Mann-Whitney tests were used for small sample sizes. * P value <0.05, $^{**}P$ value <0.01, $^{***}P$ value <0.001. Representative blot images are shown in greyscale black on white format.
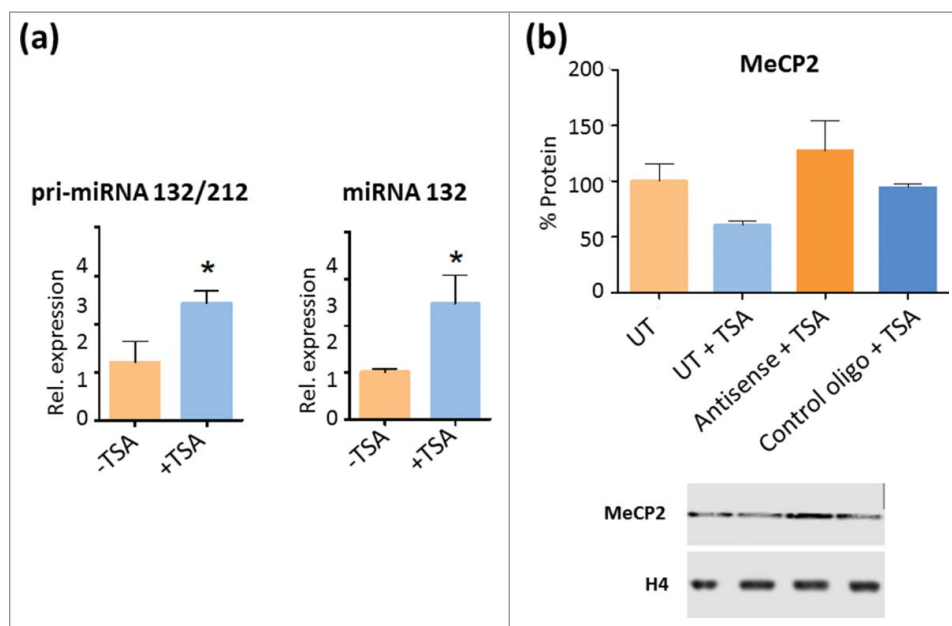
Figure 6. TSA treatment increases miR132 levels and affects MeCP2 protein levels in NIH/3T3 cells (a) Unprocessed pri-miR132/212 and mature miR132 transcription increases in TSA treated NIH/3T3 cells. Values were collected via quantitative RT-PCR. Data presented as mean $\pm$ SEM of 3–5 independent experiments. Mann-Whitney tests were used to calculate significance; * P value <0.05, ** P value <0.01, *** P value <0.001. (b) Densitometric analysis and representative WB showing MeCP2 protein levels after transfection of NIH/3T3 with an LNA oligonucleotide against miR132 MRE located in the 3′UTR of MeCP2 mRNA and a LNA oligonucleotide control upon TSA treatment.

Figure 6a shows that TSA-treated NIH/3T3 cells exhibit a significant upregulation of the pri-miR132/212, therefore resulting in the presence of higher levels of mature miR132. To verify if this upregulation directly affects MeCP2 protein levels we blocked the miR132 recognition element (MRE) in the MeCP2 3′ UTR as described before.[43] To this end, we transfected NIH/3T3 with a locked nucleic acid (LNA) oligonucleotide complementary to the MRE and an LNA control, complementary to a non-MRE sequence, also present in the MeCP2 3′ UTR.[43] Cells transfected with the specific LNA showed increased MeCP2 levels upon TSA treatment as compared to untransfected and control LNA cells (Fig. 6b). The control LNA could possibly be affecting MeCP2 mRNA stability in our system, since we observed higher levels of MeCP2

compared with untransfected TSA-treated cells. Nevertheless, our results are in agreement with a role of miR132 in the downregulation of MeCP2. Hence, overexpression of miR132 upon TSA treatment appears to be responsible for the decreased MeCP2 protein levels through a mechanism that would resemble that described in neuronal systems[43] (Fig. 7). However, we cannot rule out the possibility of other additional regulatory mechanisms also involved.

Discussion

Because of their peculiar chromatin organization in well-defined dense nuclear chromocenters, mouse NIH/3T3 cells
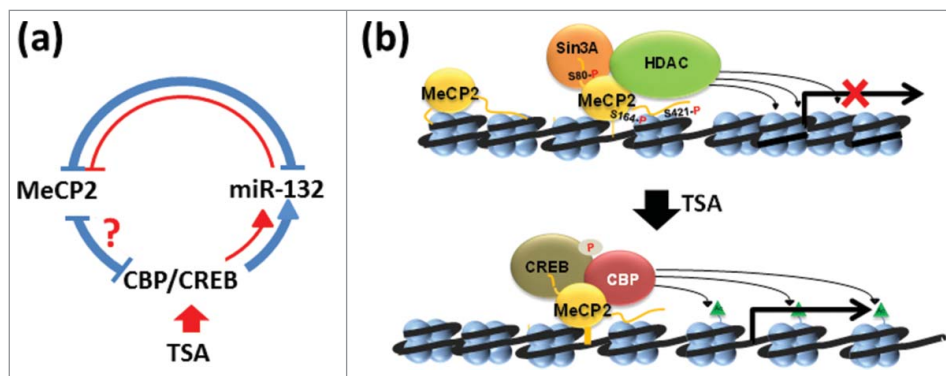

Figure 7. Model representation of the effects of HDAC inhibitors (TSA) on MeCP2 metabolism. (a) In the brain, MeCP2 expression is regulated by a complex regulatory loop 94 (shown in blue; see text for a detailed description). In red we are highlighting the regions of this network that we have been able to confirm in NIH/3T3 non-neuronal cells. (b) Based on early models of MeCP2 function, interaction of MeCP2 with an HDAC-Sin3A complex results in deacetylation of histones on surrounding nucleosomes leading to chromatin organization repressive to transcription 51. Under physiological conditions, MeCP2 is phosphorylated at several residues (S80),72 (S164),66, 72 and (S421)65 that fine-tune its transcriptional regulatory nature67, 71. Upon exposure to HDAC inhibitors such as TSA, the levels of MeCP2 phosphorylation decrease and so do the levels of the protein itself. This decrease is likely mediated by the action of CREB-CBP binding to MeCP2, which, upon acetylation of the neighboring nucleosomes (green triangles), creates a relaxed/transcriptionally-permissive chromatin organization that enhances transcription of miR132/212 4 and creates a regulatory loop of MeCP2 expression,43 shown in (a).

provide a very good model to study the nuclear distribution of MeCP2.[60] Under normal conditions, MeCP2 concentrates in these condensed heterochromatin regions.[60,75] These regions correspond to pericentromeric domains and arise from the coalescence of major satellite DNA regions with minor satellites associated with their periphery and exhibit different micrococcal nuclease sensitivity. Moreover, both regions contain the methylated forms of H3K9 and the minor satellites exhibit a relaxed chromatin organization compared to the highly compacted major type, which interacts with heterochromatin protein 1α (HP1α).[59] It is likely that the minor satellite domains are more prone to become disorganized by TSA treatment further enhancing their nuclease sensitivity in agreement with the results observed in Fig. 1 (b).

Our previous analyses on the chromatin distribution of MeCP2 in cells treated with sodium butyrate indicated that the chromatin reorganization that takes place upon such treatment does not affect the partitioning of MeCP2,[47] as observed in the MeCP2 lane of (Fig. 1c). This means that, despite the loss of chromocenter compaction upon TSA exposure [Fig. 1a TSA (C)], the remaining MeCP2 stays bound to the same chromatin territories and it exchanges from them with very similar dynamics (Fig. 2a). In addition, the elevated presence of MeCP2 in the highly nuclease accessible SI fraction of different cell types and tissues (see[3] and Fig. 1c) makes it tempting to speculate a particular type of association of MeCP2 to the minor satellite regions of the chromocenters. This may provide a hint to the massive presence of MeCP2 in the SI chromatin fraction of all organisms and cell types studied to date[76] and whose molecular explanation remains a mystery.[1] It would be interesting to know which regions of DNA are partially depleted of MeCP2 as a result of TSA treatment. Interestingly, the changes in chromatin reorganization and the more relaxed chromatin conformation adopted upon TSA treatment (Fig. 1a–b) are accompanied by a seemingly counterintuitive increase in the levels of repressive marks, such as H3K9me2 and H3K27me3, as well as the H3K4me3 activating mark, which is most likely the result of changes in gene expression resulting from TSA treatment.[77,78] In agreement with this observation, a very recent paper has shown that the increase in nuclear histone acetylation upon treatment of barley pollen with TSA also results in a nuclear accumulation of H3K27me3 and H3K4me2.[79] Such indiscriminate accumulation of histone methylation marks is most likely the result of the upregulation of histone methyltransferases by TSA treatment.[80]

Besides increasing global histone acetylation, TSA exposure alters the binding characteristics of MeCP2. It is interesting to compare the results obtained here with those obtained for histone H1 under similar TSA treatment conditions.[81] There is a striking similarity with which both chromosomal proteins compete with each other[7,82] for presumably similar in vivo binding sites[6] and for chromatinized DNA templates in vitro.[50,83] This is despite the preference of MeCP2 for methylated CpN (where N = G, A, T or C)[2] DNA regions, which are prevalent at chromatin linker regions[84,85] where linker histones (H1) bind. Our data (Fig. 3) clearly shows enhanced ionic strength-dependent binding affinity of MeCP2 to chromatin upon TSA treatment, which contrasts with the unchanged binding affinity observed under the same conditions for histone H1.[16] Nevertheless,

contrarily to histone H1,[86] TSA did not affect the binding kinetics of MeCP2 to chromatin (Fig. 2). This may simply reflect the fact that while histone acetylation has been shown to alter histone H1 binding back to acetylated chromatin once it has dissociated,[87] that of MeCP2 remains unchanged.[47] The increased binding affinity of MeCP2 upon treatment with HDAC inhibitors cannot be attributed to the overall increase in histone acetylation of nucleosomes as the binding of MeCP2 to nucleosomes in vitro has been shown to be unaffected by their extent of histone acetylation.[47]

One of the potential contributors to the TSA-induced increase in binding affinity of MeCP2 just described could be the result of a decrease in the phosphorylation of this protein due to kinase dysregulation ensuing from the HDAC inhibitors treatment. Global MeCP2 phosphorylation has been described to decrease its chromatin binding affinity.[69,88] and TSA has been shown to downregulate cdk4, cdk6, and cdk2[70] and Calcium/calmodulin-dependent protein kinase II (CaMKII).[89] MeCP2 S421-P is mediated by CaMKII[72,90] and MeCP2 S80-P is mediated by homeodomain-interacting protein kinase 2 (HIPK2).[91] Figure 4 shows that in our hand, neither one of these two phosphorylations were significantly affected by the treatment of NIH/3T3 cells with TSA. However, phosphorylation of S164 was reduced by half. Phosphorylation of S164 is a very abundant MeCP2 PTM recently described to decrease the binding affinity of MeCP2 for chromatin and to be involved in the control of dendrite patterning.[66] Although the kinase responsible is still not known, it is plausible to think that it could be a member of the cdk family. For instance, alterations in the kinase cdkl5 lead to Rett syndrome phenotypes, as is the case for MeCP2.[92] Moreover, cdkl5 has been involved in dendrite development.[93] While in the context of NIH/3T3 cells these functions may lack relevance, the fact that CDKs are also downregulated by TSA treatment and that they share neurological pathways with S164 phosphorylation, suggest that CDKL5 could be a likely candidate.

Regardless of the above chromatin structural considerations, we found that treatment of cells with TSA lead to a decrease in the overall content of nuclear MeCP2 (Fig. 5), as previously observed via treatment of HeLa cells with sodium butyrate.[47] Human HeLa, HEK293, and mouse NIH/3T3 cell lines were used (Fig. 1a–b) to corroborate those preliminary results using different germ layers and/or species.

In the brain, where most information is available for MeCP2 metabolism, CREB-CBP, MeCP2, and miR132/212 have been shown to be connected through a regulatory network (Fig. 7a) that is responsible for maintaining MeCP2 homeostasis.[94] HDAC inhibitors enhance the activation of genes regulated by the CREB-CBP transcriptional complex,[95] including miR132,[43] which represses MeCP2 levels in rat neurons[46] [see blue loop in Fig. 7a]. The results obtained here (Fig. 6) clearly support the notion of a similar regulatory feedback loop [red lines in Fig. 7a] occurring in non-neuronal cells.

As stated in the introduction, our work shows that the relationship between histone acetylation and MeCP2 is much more complex than originally anticipated. In earlier studies, mainly repressive models for the function of MeCP2,[50] antagonism was observed between the presence of MeCP2 and histone acetylation.[6] However, there is now abundant evidence in support

of a transcriptional regulatory role, wherein MeCP2 can also bind to activator complexes such as CREB-CBP[4] [see Fig.7b]. TSA, as well as other HDAC inhibitors, by decreasing the phosphorylation of MeCP2 may enhance the binding of these activator complexes to promoters (Fig. 7b), underscoring, at any rate, the larger than envisioned complexity of the relationship between histone acetylation and MeCP2 on their shared chromatin substrate.

To conclude, this work was based on an observation made in our lab several years ago: that HDAC inhibitor-induced hyperacetylation of histones in non-neuronal cells resulted in significant decrease in the levels of MeCP2.[47] A follow up to that observation here shows that HDAC inhibitor treatment results in increased MeCP2 chromatin binding affinity, which appears to be affected by a global decrease in MeCP2-S164 phosphorylation and is accompanied by significant decrease in the levels of MeCP2, in part involving miR132.

Materials and methods

Cell culture

NIH/3T3, HEK293, and HeLa S3 cells were grown at 37°C in 5% CO_2 atmosphere in Dulbecco's modified essential medium (DMEM) (Sigma-Aldrich, St. Louis, MO, USA) containing 10% bovine growth serum (BGS) (VWR, Radnor, PA, USA), 1% penicillin and streptomycin (10,000 UI and 100 mg/mL, respectively) (Sigma-Aldrich, St. Louis, MO, USA), and 1X Gibco GlutaMAX (ThermoFisher Scientific Inc., Waltham, MA, USA).

Cells were grown to high density according to ATCC standards, media was removed, plates washed in phosphate buffered saline (PBS) and cells were either treated with Trichostatin A (TSA) (Sigma-Aldrich, St. Louis, MO, USA) or new medium was added to control plates. Treatment concentrations and times used were based on both literature and/ or time-course experiments (data not shown)[61,96] and were as follows: NIH/ 3T3: 100 ng/mL (330 nM) for 24 hours; HeLa S3: 40 ng/mL (132 nM) for 12 hours; and HEK293: 120 ng/mL (396 nM) for 18 hours.

Sample preparation

Cells were harvested by removing media from plates on ice, washing with cold PBS then dislsodged by trypsinization. Trypsin was neutralized with medium (see "Cell Culture"), and samples were pelleted at 4°C for 2 minutes at 1,000 × g. Cell pellets were homogenized in 4 volumes (w/v) of cell lysis buffer (0.25 M Sucrose, 60 mM KCl, 15 mM NaCl, 10 mM MES, 5 mM $MgCl_2$, 1 mM $CaCl_2$, 0.8% Triton X-100), incubated on ice for 5 minutes, then centrifuged at 4°C for 10 minutes at 1,000 × g. The supernatant was discarded and pellets were then resuspended in a half volume of nuclei resuspension buffer (50 mM NaCl, 10 mM Pipes pH 6.8, 5 mM $MgCl_2$, 1 mM $CaCl_2$). Complete protease cocktail inhibitor (Roche Molecular Biochemicals, Laval, Quebec, Canada) was added at each step at a dilution of 1:100, as was phosphatase inhibitor cocktail (Roche Molecular Biochemicals, Laval, Quebec, Canada) at a dilution of 1:10 in the case of probing for protein phosphorylation. SDS-PAGE sample buffer (125 mM Tris HCl pH 6.8, 2% SDS. 20% glycerol, 1.43 M β-mercaptoethanol, 0.2% bromophenol blue) was added to samples, which were then sonicated in 10-second intervals for approximately 1 minute and then boiled for 60–90 seconds at 95°C. Samples were flash frozen in liquid nitrogen and stored at −80°C until use.

Chromatin fractionation

Nuclei were prepared as described in "Sample preparation" for the MNase digestions. MNase digestion for chromatin fractionation (30 U/mg of DNA) was carried out for 15 minutes on pre-warmed samples at 37°C with shaking (in a water bath) and for time-course chromatin accessibility (5 U/mg of DNA) was performed for 0, 4, 8, 12, and 16-minutes time intervals. The activity of MNase was stopped using 20 mM EDTA (pH 8.0). Chromatin fractionation was then carried out according to.[3] In brief, samples were centrifuged at 10,000 × g for 10 minutes at 4°C. Supernatants (SI) were removed and pellets were resuspended harshly and vortexed in 0.25 mM EDTA (volume equal to Buffer B), then tumbled at 4°C for 60 minutes. The pellets containing 0.25 mM EDTA were centrifuged at 16,000 × g for 10 minutes at 4°C. Supernatants (SE) were recovered and appropriate volumes of SDS sample buffer were added to the resulting pellets (P), S1 and SE, and samples were sonicated before electrophoresis.

DNA extraction

Time course MNase digested samples were supplemented with a 1:1 ratio of Protein K digestion buffer (600 mM NaCl, 40 mM EDTA, 20 mM Tris pH 7.5, 1% SDS), treated with 50 μg/ml of RNase (10 mg/ml) at 37°C for 1 h and subsequently with Proteinase K (1 μg/10 μg of DNA) for another hour at 37°C. An equal volume of Phenol:Chloroform:Isoamylic alcohol (PCI) (25:24:1) was added and samples were vortexed and centrifuged at 16,000 × g at room temperature for 10 minutes. The top aqueous layer was removed and the PCI step was repeated once more. One volume of Chloroform:Isoamyl alcohol was added to the aqueous layer, vortexed well, and centrifuged as above. The aqueous phase was removed and 0.1 volume of 3 M sodium acetate (pH 5.2) was added and vortexed. Overnight precipitation was then carried out in 2.5 volumes of ice-cold 95% ethanol. Samples were centrifuged at 16,000 × g at room temperature for 10 minutes and the supernatant was discarded. Pellets were then gently washed with same volume of 75% ethanol and centrifuged as above. The resulting pellet was then allowed to air dry and dissolved in a small volume of Tris-EDTA (TE) buffer (pH 8.0) (10 mM Tris-HCl, 1 mM EDTA). DNA concentrations were determined using NanoDrop and analyzed on 1.5% agarose gel. DNA band intensities were measured using Image Studio Lite version 5.2 to confirm an equal amount of DNA for each time interval.

Gel electrophoresis

SDS-polyacrylamide gel electrophoresis (PAGE) (10% and 15% acrylamide) were prepared as previously described.[97]

Western blot (WB)

SDS-PAGE gels were transferred for 2–3 hours at 400 mA on ice onto 0.2 μm nitrocellulose membrane (Bio-Rad, Hercules, CA, USA) in 40 mM:192 mM Tris:glycine, 20% methanol or 20 mM sodium phosphate (pH 6.8) buffer, 15% ethanol (for the analyses of PTMs). Membranes were blocked in 3% skim milk, PBS-Tween 0.1%, or 5% bovine serum albumin (BSA) in Tris-buffered saline (TBS)-Tween 0.1% (for phosphorylation) for 45 minutes at room temperature with shaking. Primary antibodies incubation was done overnight at 4°C. Primary antibodies and dilutions used were as follows: MeCP2 1:1,000 (M9317, Sigma-Aldrich, St. Louis, MO, USA), PanAcetyl H4 1:1,000 (06–866, EMD Millipore, Temecula, CA, USA), H4 1:30,000 (rabbit serum produced in-house). MeCP2 pSer80 1:1,000 (AP31635SU-N, Acris, Dunwoody Park, Atlanta GA), MeCP2 pSer164 1:1,000 (rabbit serum produced in house[66]), MeCP2 pSer421, β-actin 1:5,000 (A2228, Sigma-Aldrich, St. Louis, MO, USA), H3K9me2 1:1,000 (13969P, Cell Signaling Technologies, Danvers, MA, USA), H3K27me3 1:1,000 (07–449, EMD Millipore), H3K4me3 1:1,000 (5326P, Cell Signaling Technologies), and H3K36me3 1: 2,000 (4909P Cell Signaling Technologies). Secondary antibody incubation was carried out at room temperature for 1 hour, with three 5 minute PBS-Tween 0.1% or TBS-Tween 0.1% (for phosphorylation) washes before and afterwards. Secondary antibodies used were enhanced chemiluminescent (ECL) Anti-rabbit IgG 1:2,000 (NA934, GE Healthcare, Piscataway, NJ, USA), Donkey Anti-Sheep/Goat IgG 1:2,000 (AB324P, EMD Millipore Corporation), IRDye 800 Anti-rabbit IgG 1:10,000 (611-132-122, Rockland Antibodies & Assays, Gilbertsville, PA, USA), IRDye 680LT Anti-mouse IgG 1:20,000 (926–68020, LI-COR, Lincoln, NK, USA). The latter two secondary incubations were carried out in darkness. Western blots were acquired using Li-Cor C-digit for chemiluminescent imaging or Li-Cor Odyssey (LI-COR Biosciences) for fluorescent imaging. Images were analyzed using Li-Cor Image Studio version 5.2 software.

Fluorescence recovery after photobleaching

MeCP2-GFP plasmid and fluorescence recovery after photobleaching (FRAP) was carried out as described elsewhere.[98,99]

Salt extraction

Equal amounts of solutions of 10 mM Tris (pH 7.5), 1 mM EDTA (pH 8.0) with increasing NaCl concentration (0.4, 0.6, 0.7, 0.8, 0.9, and 1 M) were added to aliquots of TSA-treated and untreated control sample preparations (see "Sample preparation"), vortexed well, and incubated on ice for 20 minutes. Samples were then centrifuged at 4°C for 10 minutes at 16,000 $\times$ g. The supernatant was removed and appropriate volumes of SDS-PAGE sample buffer were added to both supernatants and pellets and stored at −80°C. Normalizations for WB experiments were based on equal suspension and loading volumes, determined via spectrophotometric DNA quantity analysis as well as total histone protein visualization in Coomassie-stained SDS-PAGE gels. Western blots were acquired using Li-Cor Odyssey (LI-COR Biosciences). Images were analyzed using Li-Cor Image Studio Version 5.2 software.

Immunofluorescence

NIH/3T3 cells were plated on glass coverslips (12–541B, Fisher Scientific, Pittsburgh, PA, USA) during incubation. At 24 hours TSA treatment, immunofluorescence protocol was carried out as follows: Media was removed and coverslips were washed three times in PBS-T 0.1%. Fixation was carried out in 4% paraformaldehyde for 15 min. Primary antibodies were added as follows: 1:500 for both MeCP2 and PanAcH4 (see "Western blot") in PBS-T 0.1%. This was followed by an overnight incubation at 4°C and subsequent wash 3 times in PBS-T 0.1% prior to the addition of secondary antibodies, donkey anti-rabbit Alexa 555 and donkey anti-mouse Alexa 488, both at 1:1000. The secondary antibodies were incubated for 1 hour at room temperature followed by 3 washes in PBS-T 0.1% and mounted in Immumount to view.

RNA extraction and RT-qPCR

NIH/3T3 total RNA purification was performed using TRIzol reagent (Invitrogen) following manufacturer instructions. To assess pri-miR132/212 expression, RNA was reverse-transcribed using High-Capacity cDNA Reverse Transcription Kit (Applied Biosystems). Each PCR was carried out in triplicate using SYBR Green PCR Master Mix (Applied Biosystems). Primers used are: Mecp2[98]; pri-miR132/212 (fwd: CGGTGACTCAGCCTA-GATGG, rv: GGACGGGACAGGGAAGGG[100]). To confirm reproducibility of the observed changes in transcripts levels, three different housekeeping genes were analyzed: Gapdh (fwd: AAGGTCATCCCTGAGCTGAACGGG, rv: CCAGGAAAT-GAGCTTGACAAAGTG), Ppia (fwd: CAAATGCTGGAC-CAAACACAAACG, rv: GTTCATGCCTTCTTTCACCTTCCC) and Tbp (fwd: CCCCACAACTCTTCCATTCT, rv: GCAG-GAGTGATAGGGGTCAT). Representative figures used were Mecp2/Gapdh (Fig. 5) and pri-miR132/212/Tbp (Fig. 6).

Mature miR132 reverse-transcription and RT qPCR were carried out using the TaqMan microRNA Assays #000457 (miR132-3p) and #001973 (endogenous control U6 snRNA), TaqMan microRNA Reverse Transcription kit and TaqMan Universal Master Mix II (Applied Biosystems). In all cases, thermocycling conditions were 10 minutes at 95°C, then 40 cycles of 15 seconds at 95°C and 1 minute at 60°C. Fluorescent signals were acquired by the Stratagene Mx3005P qPCR System (Agilent Technologies). Relative mRNA levels were calculated using the comparative C_t method ($\Delta\Delta C_t$), considering PCR efficiency. Fold change is equal to $10^{\Delta\Delta Ct/m}$, where 'm' is the average slope of the calibration curves for the gene of interest and the endogenous control.

Locked nucleic acid (LNA) assay

In a 6-well plate, NIH/3T3 cells at 70–80% confluency were transfected with control and antisense LNA oligos [Antisense, 5′- TAAC<u>A</u>G<u>T</u>CCTGGT<u>G</u>ATA<u>T</u>TTGG<u>T</u>CA-3′; Control, 5′- TGTA<u>G</u>AC<u>A</u>A<u>T</u>AATG<u>T</u>CC<u>A</u>TGGC<u>C</u>TT-3′ (modified bases are underlined)] at a concentration of 10 nM using

lipofectamine 3000 plus (Invitrogen), as per manufacturer's protocol. After 4 hours of transfection, the cells were treated with 100 ng/mL (330 nM) of TSA for 24 hours. This was followed by SDS preparation of protein lysate for immunoblot assays as mentioned above (see "Sample preparation").

Acknowledgments

Author contributions

KVG, AMDP, AAT, GS, MSC, MT, OK, TLG, and KM performed the experiments. BC, AU and MH designed the experiments and contributed to the discussions in the paper. NL provided reagents and contributed to the writing of the manuscript. JA conceived and wrote the manuscript.

Competing financial interests

All authors declare no competing financial interests.

References

1. Ausio J. MeCP2 and the enigmatic organization of brain chromatin. Implications for depression and cocaine addiction. Clin Epigenetics. 2016;8:58. doi:10.1186/s13148-016-0214-5. PMID:27213019

2. Gabel HW, Kinde B, Stroud H, Gilbert CS, Harmin DA, Kastan NR, Hemberg M, Ebert DH, Greenberg ME. Disruption of DNA-methylation-dependent long gene repression in Rett syndrome. Nature. 2015;522:89-93. doi:10.1038/nature14319. PMID:25762136

3. Thambirajah AA, Ng MK, Frehlick LJ, Li A, Serpa JJ, Petrotchenko EV, Silva-Moreno B, Missiaen KK, Borchers CH, Adam Hall J, et al. MeCP2 binds to nucleosome free (linker DNA) regions and to H3K9/H3K27 methylated nucleosomes in the brain. Nucleic Acids Res. 2011;40:2884-97. doi:10.1093/nar/gkr1066. PMID:22144686

4. Chahrour M, Jung SY, Shaw C, Zhou X, Wong ST, Qin J, Zoghbi HY. MeCP2, a key contributor to neurological disease, activates and represses transcription. Science. 2008;320:1224-9. doi:10.1126/science.1153252. PMID:18511691

5. Yasui DH, Peddada S, Bieda MC, Vallero RO, Hogart A, Nagarajan RP, Thatcher KN, Farnham PJ, Lasalle JM. Integrated epigenomic analyses of neuronal MeCP2 reveal a role for long-range interaction with active genes. Proc Natl Acad Sci U S A. 2007;104:19416-21. doi:10.1073/pnas.0707442104. PMID:18042715

6. Skene PJ, Illingworth RS, Webb S, Kerr AR, James KD, Turner DJ, Andrews R, Bird AP. Neuronal MeCP2 is expressed at near histone-octamer levels and globally alters the chromatin state. Mol Cell. 2010;37:457-68. doi:10.1016/j.molcel.2010.01.030. PMID:20188665

7. Ausió J, de Paz A, Esteller M. MeCP2: the long trip from a chromatin protein to neurological disorders. Trends Mol Med. 2014;20:487-98. doi:10.1016/j.molmed.2014.03.004. PMID:24766768

8. Zoghbi HY. Rett Syndrome and the ongoing legacy of close clinical observation. Cell. 2016;167:293-7. doi:10.1016/j.cell.2016.09.039. PMID:27716498

9. Ballestar E, Paz MF, Valle L, Wei S, Fraga MF, Espada J, Cigudosa JC, Huang TH, Esteller M. Methyl-CpG binding proteins identify novel sites of epigenetic inactivation in human cancer. Embo J. 2003;22:6335-45. doi:10.1093/emboj/cdg604. PMID:14633992

10. Lopez-Serra L, Ballestar E, Fraga MF, Alaminos M, Setien F, Esteller M. A profile of methyl-CpG binding domain protein occupancy of hypermethylated promoter CpG islands of tumor suppressor genes in human cancer. Cancer Res 2006;66:8342-6. doi:10.1158/0008-5472.CAN-06-1932. PMID:16951140

11. Baylin SB, Jones PA. Epigenetic Determinants of Cancer. Cold Spring Harb Perspect Biol 2016;8(9). doi:10.1101/cshperspect.a019505. PMID:27194046

12. Leonhardt H, Cardoso MC. DNA methylation, nuclear structure, gene expression and cancer. J Cell Biochem Suppl. 2000;Suppl 35:78-83. doi:10.1002/1097-4644(2000)79:35+<78::AID-JCB1129>3.0.CO;2-J. PMID:11389535

13. Neupane M, Clark AP, Landini S, Birkbak NJ, Eklund AC, Lim E, Culhane AC, Barry WT, Schumacher SE, Beroukhim R, et al. MECP2 Is a Frequently Amplified Oncogene with a Novel Epigenetic Mechanism that Mimics the Role of Activated RAS in Malignancy. Cancer Discov. 2015;6(1):45-58. PMID:26546296

14. Garcia Ramirez M, Rocchini C, Ausió J. Modulation of chromatin folding by histone acetylation. J Biol Chem. 1995;270:17923-8. doi:10.1074/jbc.270.30.17923. PMID:7629098

15. Wakamori M, Fujii Y, Suka N, Shirouzu M, Sakamoto K, Umehara T, Yokoyama S. Intra- and inter-nucleosomal interactions of the histone H4 tail revealed with a human nucleosome core particle with genetically-incorporated H4 tetra-acetylation. Sci Rep. 2015;5:17204. doi:10.1038/srep17204. PMID:26607036

16. Wang X, He C, Moore SC, Ausió J. Effects of histone acetylation on the solubility and folding of the chromatin fiber. J Biol Chem. 2001;276:12764-8. doi:10.1074/jbc.M100501200. PMID:11279082

17. Calestagne-Morelli A, Ausio J. Long-range histone acetylation: biological significance, structural implications, and mechanisms. Biochem Cell Biol. 2006;84:518-27. doi:10.1139/o06-067. PMID:16936824

18. Ausió J, Abbott DW. The role of histone variability in chromatin stability and folding. Amsterdam, The Netherlands: Elsevier; 2004.p. 241-90.

19. Zago V, Pinar-CabezaDeVaca C, Vincent JB, Ausio J. Histone variants and composition in the developing brain: should MeCP2 care? Curr Top Med Chem. 2016;17(7):829–42. PMID:27086783

20. Mitrousis N, Tropepe V, Hermanson O. Post-Translational Modifications of Histones in Vertebrate Neurogenesis. Front Neurosci. 2015;9:483. doi:10.3389/fnins.2015.00483. PMID:26733796

21. Bonnaud EM, Suberbielle E, Malnou CE. Histone acetylation in neuronal (dys)function. Biomol Concepts. 2016;7:103-16. doi:10.1515/bmc-2016-0002. PMID:27101554

22. Yoshida M, Furumai R, Nishiyama M, Komatsu Y, Nishino N, Horinouchi S. Histone deacetylase as a new target for cancer chemotherapy. Cancer Chemother Pharmacol. 2001;48 Suppl 1:S20-6. doi:10.1007/s002800100300. PMID:11587361

23. Johnstone RW. Histone-deacetylase inhibitors: novel drugs for the treatment of cancer. Nat Rev Drug Discov. 2002;1:287-99. doi:10.1038/nrd772. PMID:12120280

24. La Thangue NB. Histone deacetylase inhibitors and cancer therapy. J Chemother. 2004;16 Suppl 4:64-7. doi:10.1179/joc.2004.16.Supplement-1.64. PMID:15688613

25. Dokmanovic M, Clarke C, Marks PA. Histone deacetylase inhibitors: overview and perspectives. Mol Cancer Res. 2007;5:981-9. doi:10.1158/1541-7786.MCR-07-0324. PMID:17951399

26. Noureen N, Rashid H, Kalsoom S. Identification of type-specific anti-cancer histone deacetylase inhibitors: road to success. Cancer Chemother Pharmacol. 2010;66:625-33. doi:10.1007/s00280-010-1324-y. PMID:20401613

27. Khan O, La Thangue NB. HDAC inhibitors in cancer biology: emerging mechanisms and clinical applications. Immunol Cell Biol. 2012;90:85-94. doi:10.1038/icb.2011.100. PMID:22124371

28. Delcuve GP, Khan DH, Davie JR. Targeting class I histone deacetylases in cancer therapy. Expert Opin Ther Targets. 2013;17:29-41. doi:10.1517/14728222.2013.729042. PMID:23062071

29. Hrabeta J, Stiborova M, Adam V, Kizek R, Eckschlager T. Histone deacetylase inhibitors in cancer therapy. A review. Biomed Pap Med Fac Univ Palacky Olomouc Czech Repub. 2014;158:161-9.

30. Zhang L, Han Y, Jiang Q, Wang C, Chen X, Li X, Xu F, Jiang Y, Wang Q, Xu W. Trend of histone deacetylase inhibitors in cancer therapy: isoform selectivity or multitargeted strategy. Med Res Rev. 2015;35:63-84. doi:10.1002/med.21320. PMID:24782318

31. Turtoi A, Peixoto P, Castronovo V, Bellahcene A. Histone deacetylases and cancer-associated angiogenesis: current understanding of

the biology and clinical perspectives. Crit Rev Oncog. 2015;20:119-37. doi:10.1615/CritRevOncog.2014012423. PMID:25746107

32. Li Y, Seto E. HDACs and HDAC inhibitors in cancer development and therapy. Cold Spring Harb Perspect Med. 2016;6. doi:10.1101/cshperspect.a026831. PMID:27599530

33. Damaskos C, Valsami S, Kontos M, Spartalis E, Kalampokas T, Kalampokas E, Athanasiou A, Moris D, Daskalopoulou A, Davakis S, et al. Histone deacetylase inhibitors: an attractive therapeutic strategy against breast cancer. Anticancer Res. 2017;37:35-46. doi:10.21873/anticanres.11286. PMID:28011471

34. Ganai SA, Ramadoss M, Mahadevan V. Histone Deacetylase (HDAC) Inhibitors – emerging roles in neuronal memory, learning, synaptic plasticity and neural regeneration. Curr Neuropharmacol. 2016;14:55-71. doi:10.2174/1570159X13666151021111609. PMID:26487502

35. Penney J, Tsai LH. Histone deacetylases in memory and cognition. Sci Signal. 2014;7:re12. doi:10.1126/scisignal.aaa0069. PMID:25492968

36. Falkenberg KJ, Johnstone RW. Histone deacetylases and their inhibitors in cancer, neurological diseases and immune disorders. Nat Rev Drug Discov. 2014;13:673-91. doi:10.1038/nrd4360. PMID:25131830

37. Fischer A, Sananbenesi F, Mungenast A, Tsai LH. Targeting the correct HDAC(s) to treat cognitive disorders. Trends Pharmacol Sci. 2010;31:605-17. doi:10.1016/j.tips.2010.09.003. PMID:20980063

38. Chuang DM, Leng Y, Marinova Z, Kim HJ, Chiu CT. Multiple roles of HDAC inhibition in neurodegenerative conditions. Trends Neurosci. 2009;32:591-601. doi:10.1016/j.tins.2009.06.002. PMID:19775759

39. Echaniz-Laguna A, Bousiges O, Loeffler JP, Boutillier AL. Histone deacetylase inhibitors: therapeutic agents and research tools for deciphering motor neuron diseases. Curr Med Chem. 2008;15:1263-73. doi:10.2174/092986708784534974. PMID:18537606

40. Langley B, Gensert JM, Beal MF, Ratan RR. Remodeling chromatin and stress resistance in the central nervous system: histone deacetylase inhibitors as novel and broadly effective neuroprotective agents. Curr Drug Targets CNS Neurol Disord. 2005;4:41-50. doi:10.2174/1568007053005091. PMID:15723612

41. Bojang P, Jr, Ramos KS. The promise and failures of epigenetic therapies for cancer treatment. Cancer Treat Rev. 2014;40:153-69. doi:10.1016/j.ctrv.2013.05.009. PMID:23831234

42. Halsall JA, Turner BM. Histone deacetylase inhibitors for cancer therapy: An evolutionarily ancient resistance response may explain their limited success. Bioessays. 2016;38(11):1102-1110. doi:10.1002/bies.201600070. PMID:27717012

43. Klein ME, Lioy DT, Ma L, Impey S, Mandel G, Goodman RH. Homeostatic regulation of MeCP2 expression by a CREB-induced microRNA. Nat Neurosci. 2007;10:1513-4. doi:10.1038/nn2010. PMID:17994015

44. Hollander JA, Im HI, Amelio AL, Kocerha J, Bali P, Lu Q, Willoughby D, Wahlestedt C, Conkright MD, Kenny PJ. Striatal microRNA controls cocaine intake through CREB signalling. Nature. 2010;466:197-202. doi:10.1038/nature09202. PMID:20613834

45. Im HI, Hollander JA, Bali P, Kenny PJ. MeCP2 controls BDNF expression and cocaine intake through homeostatic interactions with microRNA-212. Nat Neurosci. 2010;13:1120-7. doi:10.1038/nn.2615. PMID:20711185

46. Chahrour M, Zoghbi HY. The story of Rett syndrome: from clinic to neurobiology. Neuron. 2007;56:422-37. doi:10.1016/j.neuron.2007.10.001. PMID:17988628

47. Ishibashi T, Thambirajah AA, Ausio J. MeCP2 preferentially binds to methylated linker DNA in the absence of the terminal tail of histone H3 and independently of histone acetylation. FEBS Lett. 2008;582:1157-62. doi:10.1016/j.febslet.2008.03.005. PMID:18339321

48. Host L, Dietrich JB, Carouge D, Aunis D, Zwiller J. Cocaine self-administration alters the expression of chromatin-remodelling proteins; modulation by histone deacetylase inhibition. J Psychopharmacol. 2011;25:222-9. doi:10.1177/0269881109348173. PMID:19939859

49. Ghoshal K, Datta J, Majumder S, Bai S, Dong X, Parthun M, Jacob ST. Inhibitors of histone deacetylase and DNA methyltransferase synergistically activate the methylated metallothionein I promoter by activating the transcription factor MTF-1 and forming an open

chromatin structure. Mol Cell Biol. 2002;22:8302-19. doi:10.1128/MCB.22.23.8302-8319.2002. PMID:12417732

50. Nan X, Campoy FJ, Bird A. MeCP2 is a transcriptional repressor with abundant binding sites in genomic chromatin. Cell. 1997;88:471-81. doi:10.1016/S0092-8674(00)81887-5. PMID:9038338

51. Nan X, Ng HH, Johnson CA, Laherty CD, Turner BM, Eisenman RN, Bird A. Transcriptional repression by the methyl-CpG-binding protein MeCP2 involves a histone deacetylase complex. Nature. 1998;393:386-9. doi:10.1038/30764. PMID:9620804

52. Eden S, Hashimshony T, Keshet I, Cedar H, Thorne AW. DNA methylation models histone acetylation. Nature. 1998;394:842. doi:10.1038/29680. PMID:9732866

53. Ballestar E, Esteller M. The epigenetic breakdown of cancer cells: from DNA methylation to histone modifications. Prog Mol Subcell Biol. 2005;38:169-81. doi:10.1007/3-540-27310-7_7. PMID:15881895

54. Ballestar E, Esteller M. Methyl-CpG-binding proteins in cancer: blaming the DNA methylation messenger. Biochem Cell Biol. 2005;83:374-84. doi:10.1139/o05-035. PMID:15959563

55. Ou JN, Torrisani J, Unterberger A, Provencal N, Shikimi K, Karimi M, Ekstrom TJ, Szyf M. Histone deacetylase inhibitor Trichostatin A induces global and gene-specific DNA demethylation in human cancer cell lines. Biochem Pharmacol. 2007;73:1297-307. doi:10.1016/j.bcp.2006.12.032. PMID:17276411

56. Kim HJ, Bae SC. Histone deacetylase inhibitors: molecular mechanisms of action and clinical trials as anti-cancer drugs. Am J Transl Res. 2011;3:166-79. PMID:21416059

57. Vanhaecke T, Papeleu P, Elaut G, Rogiers V. Trichostatin A-like hydroxamate histone deacetylase inhibitors as therapeutic agents: toxicological point of view. Curr Med Chem. 2004;11:1629-43. doi:10.2174/0929867043365099. PMID:15180568

58. Mateos-Langerak J, Brink MC, Luijsterburg MS, van der Kraan I, van Driel R, Verschure PJ. Pericentromeric heterochromatin domains are maintained without accumulation of HP1. Mol Biol Cell. 2007;18:1464-71. doi:10.1091/mbc.E06-01-0025. PMID:17314413

59. Guenatri M, Bailly D, Maison C, Almouzni G. Mouse centric and pericentric satellite repeats form distinct functional heterochromatin. J Cell Biol. 2004;166:493-505. doi:10.1083/jcb.200403109. PMID:15302854

60. Hu K, Nan X, Bird A, Wang W. Testing for association between MeCP2 and the brahma-associated SWI/SNF chromatin-remodeling complex. Nat Genet. 2006;38:962-4; author reply 4–7. doi:10.1038/ng0906-962. PMID:16940996

61. Felisbino MB, Gatti MS, Mello ML. Changes in chromatin structure in NIH 3T3 cells induced by valproic acid and trichostatin A. J Cell Biochem. 2014;115:1937-47. doi:10.1002/24913611. PMID:24913611

62. Ishibashi T, Dryhurst D, Rose KL, Shabanowitz J, Hunt DF, Ausio J. Acetylation of vertebrate H2A.Z and its effect on the structure of the nucleosome. Biochemistry. 2009;48:5007-17. doi:10.1021/bi900196c. PMID:19385636

63. Kumar A, Kamboj S, Malone BM, Kudo S, Twiss JL, Czymmek KJ, LaSalle JM, Schanen NC. Analysis of protein domains and Rett syndrome mutations indicate that multiple regions influence chromatin-binding dynamics of the chromatin-associated protein MECP2 in vivo. J Cell Sci. 2008;121:1128-37. doi:10.1242/jcs.016865. PMID:18334558

64. Lever MA, Th'ng JP, Sun X, Hendzel MJ. Rapid exchange of histone H1.1 on chromatin in living human cells. Nature. 2000;408:873-6. doi:10.1038/35048603. PMID:11130728

65. Zhou Z, Hong EJ, Cohen S, Zhao WN, Ho HY, Schmidt L, Chen WG, Lin Y, Savner E, Griffith EC, et al. Brain-specific phosphorylation of MeCP2 regulates activity-dependent Bdnf transcription, dendritic growth, and spine maturation. Neuron. 2006;52:255-69. doi:10.1016/j.neuron.2006.09.037. PMID:17046689

66. Stefanelli G, Gandaglia A, Costa M, Cheema MS, Di Marino D, Barbiero I, Kilstrup-Nielsen C, Ausio J, Landsberger N. Brain phosphorylation of MeCP2 at serine 164 is developmentally regulated and globally alters its chromatin association. Sci Rep. 2016;6:28295. doi:10.1038/srep28295. PMID:27323888

67. Bellini E, Pavesi G, Barbiero I, Bergo A, Chandola C, Nawaz MS, Rusconi L, Stefanelli G, Strollo M, Valente MM, et al. MeCP2 post-

translational modifications: a mechanism to control its involvement in synaptic plasticity and homeostasis? Front Cell Neurosci. 2014;8:236. doi:10.3389/fncel.2014.00236. PMID:25165434

68. Cohen S, Gabel HW, Hemberg M, Hutchinson AN, Sadacca LA, Ebert DH, Harmin DA, Greenberg RS, Verdine VK, Zhou Z, et al. Genome-wide activity-dependent MeCP2 phosphorylation regulates nervous system development and function. Neuron. 2011;72:72-85. doi:10.1016/j.neuron.2011.08.022. PMID:21982370

69. Chen WG, Chang Q, Lin Y, Meissner A, West AE, Griffith EC, Jaenisch R, Greenberg ME. Derepression of BDNF transcription involves calcium-dependent phosphorylation of MeCP2. Science. 2003;302:885-9. doi:10.1126/science.1086446. PMID:14593183

70. Milton SG, Mathew OP, Yatsu FM, Ranganna K. Differential cellular and molecular effects of butyrate and trichostatin a on vascular smooth muscle cells. Pharmaceuticals (Basel). 2012;5:925-43. doi:10.3390/ph5090925. PMID:24280698

71. Chao HT, Zoghbi HY. The yin and yang of MeCP2 phosphorylation. Proc Natl Acad Sci U S A. 2009;106:4577-8. doi:10.1073/pnas.0901518106. PMID:19293386

72. Tao J, Hu K, Chang Q, Wu H, Sherman NE, Martinowich K, Klose RJ, Schanen C, Jaenisch R, Wang W, et al. Phosphorylation of MeCP2 at Serine 80 regulates its chromatin association and neurological function. Proc Natl Acad Sci U S A. 2009;106:4882-7. doi:10.1073/pnas.0811648106. PMID:19225110

73. Sekhavat A, Sun JM, Davie JR. Competitive inhibition of histone deacetylase activity by trichostatin A and butyrate. Biochem Cell Biol. 2007;85:751-8. doi:10.1139/O07-145. PMID:18059533

74. Chao HT, Zoghbi HY. MeCP2: only 100% will do. Nat Neurosci. 2012;15:176-7. doi:10.1038/nn.3027. PMID:22281712

75. Nan X, Tate P, Li E, Bird A. DNA methylation specifies chromosomal localization of MeCP2. Mol Cell Biol. 1996;16:414-21. doi:10.1128/MCB.16.1.414. PMID:8524323

76. Thambirajah AA, Ausio J. A moment's pause: putative nucleosome-based influences on MeCP2 regulation. Biochem Cell Biol. 2009;87:791-8. doi:10.1139/O09-054. PMID:19898528

77. Lamb J, Crawford ED, Peck D, Modell JW, Blat IC, Wrobel MJ, Lerner J, Brunet JP, Subramanian A, Ross KN, et al. The Connectivity Map: using gene-expression signatures to connect small molecules, genes, and disease. Science. 2006;313:1929-35. doi:10.1126/science.1132939. PMID:17008526

78. Yeakley JM, Shepard PJ, Goyena DE, VanSteenhouse HC, McComb JD, Seligmann BE. A trichostatin A expression signature identified by TempO-Seq targeted whole transcriptome profiling. PLoS One. 2017;12:e0178302. doi:10.1371/journal.pone.0178302. PMID:28542535

79. Pandey P, Daghma DS, Houben A, Kumlehn J, Melzer M, Rutten T. Dynamics of post-translationally modified histones during barley pollen embryogenesis in the presence or absence of the epi-drug trichostatin A. Plant Reprod. 2017;30:95-105. doi:10.1007/s00497-017-0302-5. PMID:28526911

80. Sanders YY, Tollefsbol TO, Varisco BM, Hagood JS. Epigenetic regulation of thy-1 by histone deacetylase inhibitor in rat lung fibroblasts. Am J Respir Cell Mol Biol. 2011;45:16-23. doi:10.1165/rcmb.2010-0154OC. PMID:20724553

81. Raghuram N, Carrero G, Stasevich TJ, McNally JG, Th'ng J, Hendzel MJ. Core histone hyperacetylation impacts cooperative behavior and high-affinity binding of histone H1 to chromatin. Biochem. 2010;49:4420-31. doi:10.1021/bi100296z.

82. iClaveria-Gimeno R, Abian O, Velazquez-Campoy A, Ausió J. MeCP2…Nature's wonder protein or medicine's most feared one. Curr Genet Med Rep. 2016;4:180-94. doi:10.1007/s40142-016-0107-0.

83. Ghosh RP, Horowitz-Scherer RA, Nikitina T, Shlyakhtenko LS, Woodcock CL. MeCP2 binds cooperatively to its substrate and competes with histone H1 for chromatin binding sites. Mol Cell Biol. 2010;30 (19):4656-70. doi:10.1128/MCB.00379-10. PMID:20679481

84. Zhang Y, Jurkowska R, Soeroes S, Rajavelu A, Dhayalan A, Bock I, Rathert P, Brandt O, Reinhardt R, Fischle W, et al. Chromatin methylation activity of Dnmt3a and Dnmt3a/3L is guided by interaction of the ADD domain with the histone H3 tail. Nucleic Acids Res. 2010;38:4246-53. doi:10.1093/nar/gkq147. PMID:20223770

85. Felle M, Hoffmeister H, Rothammer J, Fuchs A, Exler JH, Langst G. Nucleosomes protect DNA from DNA methylation in vivo and in vitro. Nucleic Acids Res. 2011;39(16):6956-69. doi:10.1093/nar/gkr263. PMID:21622955

86. Raghuram N, Carrero G, Th'ng J, Hendzel MJ. Molecular dynamics of histone H1. Biochem Cell Biol. 2009;87:189-206. doi:10.1139/O08-127. PMID:19234534

87. Ridsdale JA, Hendzel MJ, Delcuve GP, Davie JR. Histone acetylation alters the capacity of the H1 histones to condense transcriptionally active/competent chromatin. J Biol Chem. 1990;265:5150-6. PMID:2318888

88. Martinowich K, Hattori D, Wu H, Fouse S, He F, Hu Y, Fan G, Sun YE. DNA methylation-related chromatin remodeling in activity-dependent BDNF gene regulation. Science. 2003;302:890-3. doi:10.1126/science.1090842. PMID:14593184

89. Eickhoff B, Germeroth L, Stahl C, Kohler G, Ruller S, Schlaak M, van der Bosch J. Trichostatin A-mediated regulation of gene expression and protein kinase activities: reprogramming tumor cells for ribotoxic stress-induced apoptosis. Biol Chem. 2000;381:1127-32. doi:10.1515/BC.2000.138. PMID:11154071

90. Buchthal B, Lau D, Weiss U, Weislogel JM, Bading H. Nuclear calcium signaling controls methyl-CpG-binding protein 2 (MeCP2) phosphorylation on serine 421 following synaptic activity. J Biol Chem. 2012;287:30967-74. doi:10.1074/jbc.M112.382507. PMID:22822052

91. Bracaglia G, Conca B, Bergo A, Rusconi L, Zhou Z, Greenberg M, Landsberger N, Soddu S, Kilstrup-Nielsen C. Methyl-CpG-binding protein 2 is phosphorylated by homeodomain-interacting protein kinase 2 and contributes to apoptosis. EMBO Rep. 2009;10:1327-33. doi:10.1038/embor.2009.217. PMID:19820693

92. Mari F, Azimonti S, Bertani I, Bolognese F, Colombo E, Caselli R, Scala E, Longo I, Grosso S, Pescucci C, et al. CDKL5 belongs to the same molecular pathway of MeCP2 and it is responsible for the early-onset seizure variant of Rett syndrome. Hum Mol Genet. 2005;14:1935-46. doi:10.1093/hmg/ddi198. PMID:15917271

93. Zhu YC, Li D, Wang L, Lu B, Zheng J, Zhao SL, Zeng R, Xiong ZQ. Palmitoylation-dependent CDKL5-PSD-95 interaction regulates synaptic targeting of CDKL5 and dendritic spine development. Proc Natl Acad Sci US A. 2013;110:9118-23. doi:10.1073/pnas.1300003110.

94. Feng J, Nestler EJ. MeCP2 and drug addiction. Nat Neurosci. 2010;13:1039-41. doi:10.1038/nn0910-1039. PMID:20740030

95. Vecsey CG, Hawk JD, Lattal KM, Stein JM, Fabian SA, Attner MA, Cabrera SM, McDonough CB, Brindle PK, Abel T, et al. Histone deacetylase inhibitors enhance memory and synaptic plasticity via CREB:CBP-dependent transcriptional activation. J Neurosci. 2007;27:6128-40. doi:10.1523/JNEUROSCI.0296-07.2007. PMID:17553985

96. Brown CR, Kennedy CJ, Delmar VA, Forbes DJ, Silver PA. Global histone acetylation induces functional genomic reorganization at mammalian nuclear pore complexes. Genes Dev. 2008;22:627-39. doi:10.1101/gad.1632708. PMID:18316479

97. Laemmli UK. Cleavage of structural proteins during the assembly of the head of bacteriophage T4. Nature. 1970;227:680-5. doi:10.1038/227680a0. PMID:5432063

98. Stuss DP, Cheema M, Ng MK, Martinez de Paz A, Williamson B, Missiaen K, Cosman JD, McPhee D, Esteller M, Hendzel M, et al. Impaired in vivo binding of MeCP2 to chromatin in the absence of its DNA methyl-binding domain. Nucleic Acids Res. 2013;41:4888-900. doi:10.1093/nar/gkt213. PMID:23558747

99. Carrero G, McDonald D, Crawford E, de_Vries G, Hendzel MJ. Using FRAP and mathematical modeling to determine the in vivo kinetics of nuclear proteins. Methods (San Diego, Calif). 2003;29:14-28. doi:10.1016/S1046-2023(02)00288-8. PMID:12543068

100. Remenyi J, van den Bosch MW, Palygin O, Mistry RB, McKenzie C, Macdonald A, Hutvagner G, Arthur JS, Frenguelli BG, Pankratov Y. miR-132/212 knockout mice reveal roles for these miRNAs in regulating cortical synaptic transmission and plasticity. PLoS One. 2013;8:e62509. doi:10.1371/journal.pone.0062509. PMID:23658634